JOURNAL OF CIVIL ENGINEERING AND MANAGEMENT
ISSN 1392-3730/eISSN 1822-3605
2015 Volume 21(5): 637–653
doi:10.3846/13923730.2014.890650

A PROBABILISTIC EVALUATION OF PIER-SCOUR POTENTIAL IN THE GAOPING RIVER BASIN OF TAIWAN

Kuo-Wei LIAO[a], Hu-Jhong LU[a], Chung-Yue WANG[b]

[a]*National Taiwan University of Science and Technology, No. 43, Sec. 4, Keelung Rd., Da'an Dist.,Taipei City 106, Taiwan*
[b]*National Central University, No. 300, Jhongda Rd., Taoyuan, Jhongli, 32001, Taiwan*

Received 16 Jul 2012; accepted 19 Dec 2012

Abstract. A probabilistic approach is used to create a preliminary inspection evaluation form (PIEF) for scour potential at bridge sites. In Taiwan, the risk of pier scour is often evaluated using a two-step procedure. First, a bridge is visually inspected based on a PIEF. An advanced scour risk analysis is conducted for a bridge with a high PIEF score. Because a PIEF can quickly evaluate scour potential, it can be used to build a maintenance sequence for a group of bridges. However, a PIEF is often created based on only engineers' experience; the accuracy and reliability of PIEFs have not been examined systematically. Thus, a probabilistic-based PIEF is constructed by establishing a close correlation between the PIEF score and scour potential via Taguchi method. The scour potential is evaluated by Bayesian network (BN) that incorporates experts' judgments and results of reliability analyses. For example, the conditional probabilities (CP) in the proposed BN are calculated based on an existing PIEF and results of a stability-based reliability analysis. Thus, the proposed PIEF implicitly considers the probabilistic characteristics in the scour potential, which will provide an efficient and accurate evaluation of scour potential and assist in establishing maintenance priorities of existing bridges in Taiwan.

Keywords: reliability, bridges, maintenance, scour potential.

Introduction

The scour potential at bridge sites in Taiwan has drawn much attention in recent years, especially after Typhoon Morakot in 2009. Because scour potential evaluation involves many uncertainties, a probabilistic approach is often adopted. Johnson and Ayyub (1992) used simulation method to evaluate bridge failure probability. Muzzammil *et al.* (2008) used reliability index to develop a reliability-based safety factor method for field application. There are approximately 20,000 bridges in Taiwan. A probabilistic evaluation for each bridge is not a practical solution. A preliminary inspection evaluation form (PIEF) can efficiently evaluate the scour potential of a bridge. Thus, a priority maintenance list can be built based on PIEF to effectively reduce the scour risk from future disasters. The PIEF is a visual inspection process that is generally used in Taiwan as the first step of a bridge scour risk evaluation. If the overall assessment score from the PIEF does not meet a predefined standard, the evaluation should proceed to an advanced investigation to ensure the safety of bridges.

Several scouring assessment measures using the approach of PIEF have been proposed. For example, Palmer and Turkiyyah (1997) proposed an assessment approach called Cataloging and Expert Evaluation of Scour Risk and River Stability at Bridge Sites (CAESAR). CAESAR is an expert system that uses the insights and judgments of scour experts and inspectors to generate suggestions about the possibility of scour and potential mitigation actions. In addition to CAESAR, U.S. Department of Transportation has issued three manuals: HEC-18 (U.S. Department of Transportation 2012); HEC-20 (U.S. Department of Transportation 2001a); and HEC-23 (U.S. Department of Transportation 2001b) to provide guidance for bridge scour and stream stability analyses. In Japan, to correctly and efficiently identify scouring-affected bridge piers, the Railway Technical Research Institute (RTRI) (2007) established a technique that uses two scoring tables to select bridge piers for repairs or remodeling.

In Taiwan, the first PIEF was proposed by Chen *et al.* (1996). Recently, many researchers have proposed several different PIEFs. For example, China Engineering Consultants, Inc. utilized their practical experience to develop a new PIEF as shown in Table 1, where h, D_h, θ, RA, H_s/H_p and b_e are described in Figure 1. This PIEF consists of 13 evaluated items, including 6 indoor assessment items with a total allocated score of 35 and 7 in-situ assessment items with a total allocated score of 65. Each evaluated item is allocated a weight (α in

Corresponding author: Kuo-Wei Liao
E-mail: *kliao@mail.ntust.edu.tw*

Table 1) to indicate its relative importance. The sum of all the weights is 100. In addition, each evaluated item is divided into three to five levels, and another weight (β in Table 1) is assigned to each level. If the evaluated item definitely has a positive influence on the inspected bridge, β is equal to 1. Otherwise, β is equal to 0. A value between 0 and 1 is assigned to an intermediate level of β. Thus, β and α determine the score for each evaluated item. The overall assessment score of an inspected bridge is the sum of

Table 1. The preliminary inspection evaluation form (PIEF) of China Engineering Consultants Inc.

	No.	Item	α	β
Indoor assessment item	1	Upstream river dam or reservoir facilities	7	□ within 1000 m (β = 1.0) □ 1000 m~3000 m (β = 0.5) □ 3000 m above or none (β = 0)
	2	Foundation type	7	□ shallow foundation or extended foundation footing (β = 1.0) □ cassion foundation (β = 0.5) □ pile foundation (β = 0)
	3	Bending or narrowing of the river	6	□ Yes (β = 1.0) □ No (β = 0)
	4	Eroded river bed h = m	8	*(β = 1.0) ≥ β =1– 0.75(4 – h)/3.5 ≥ (β = 0.25); h < 0.5 m, β = 0
	5	Material on the river bed	2	□ mud, sand (β = 1.0) □ sand and gravel mixture (β = 0.75) □ gravel (β = 0.5) □ soft bed rock (mudstone, shale, etc) (β =0.3) □ hard bed rock (β = 0)
	6	Location of the main channel	5	□*within 5 m from the abutment (β = 1.0) □ with 10 m from the abutment, and in the trend of erosion in the direction of the abutment by years (β = 0.5) □ braided river channels, hard to determine the main channel (β = 0.3) □ more than 10 m from the abutment or abutment foundation is indirect foundation (β = 0)
		Sum (sub-total)	35	
In-situ assessment item	7	Hydraulic drop effect (difference of height D_h = m)	5	(β = 1.0) ≥ β = D_h/3≥(β = 0)
	8	Attack angle of flow (θ°)	7	(1.0) ≥ β = (θ° – 5°)/25° ≥ (0); θ < 5°, β = 0; θ ≥ 30°, β = 1
	9	Area ratio of bridge to cross section (*RA*)	5	□ extremely serious (RA > 12%) (β = 1.0) □ serious (9% < RA < 12%) (β = 0.5) □ slight (RA< 9%) (β = 0.2) □ None (RA < 3%) (β = 0)
	10	Foundation exposure depth (*Hs*) *Hp* (initial foundation depth) *S* = *Hs*/*Hp* *Hsa* = *Hp*/4	20	cassion or pile foundation: □*$Hs \geq 1.5Hsa$ or $S \geq 40\%$ (β = 1.0) □ $1.5Hsa > Hs > 1.0Hsa$ or $40\% > S > 25\%$ (β = 0.5 ~ 0.9) □ $Hs < 1.0Hsa$ or $S < 25\%$ (β = 0.2) □ None (β = 0) Shallow foundation: □ placed in the gravel bed or *have been exposed (β = 1.0) □ to the surface of the bed rock (β = 0.5) □ deep into the bed rock (β = 0)
	11	Effective pier diameter (b_e)	13	When $b_e > 8$, β = 1.0; When $2 < b_e < 8$, β = [–1/3 + (1/6)b_e]; When $b_e < 2$, β = 0
	12	Protection for river bank	5	□ no protection (β = 1.0) □ with only partial protection (β = 0.3) □ no need to protect the river bank (β = 0) □ good protection for river bank (β = –0.2)
	13	Protection for river bed	10	□ no protection (β = 1.0) □ with only partial protection (β = 0.3) □ no need to protect the river bed (β = 0) □ good protection for river bed (β = –0.2)
		Sum (sub-total)	65	
		Total	100	

* If satisfying this condition, regardless of the overall score, the bridge is categorized as a bridge of high scouring potential.

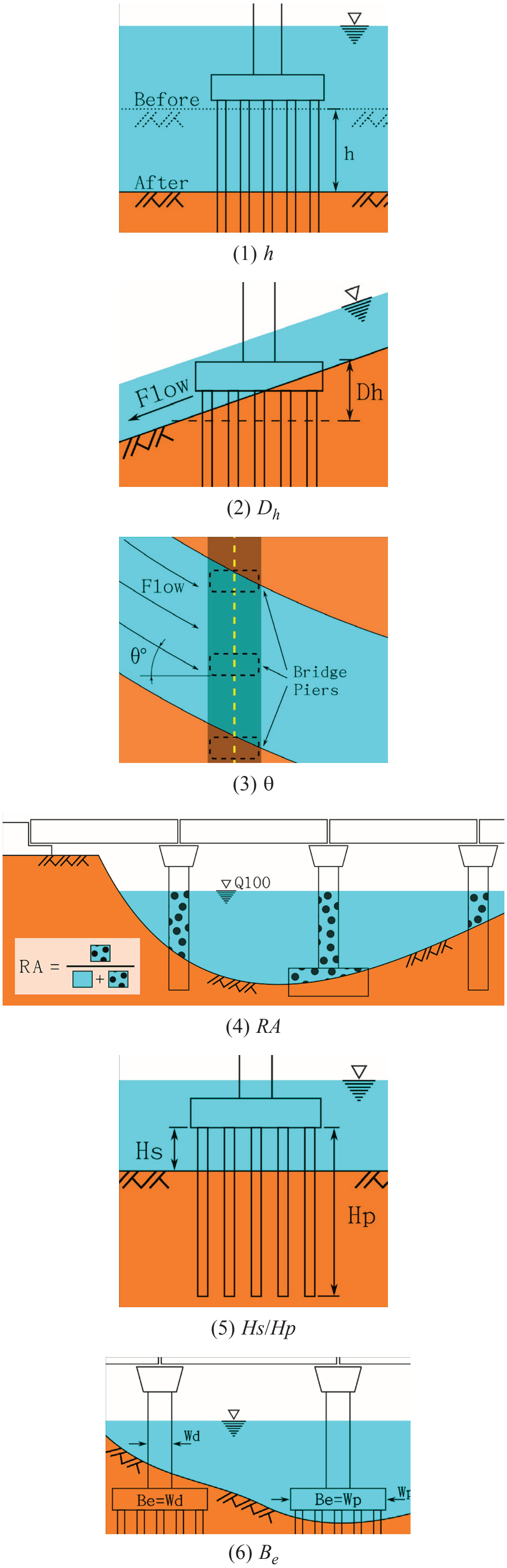

Fig. 1. Illustrations of symbols used in Table 1

the scores from each evaluated item. An overall score below 25 indicates a low scouring potential, an overall score between 25 and 50 indicates a medium scouring potential and an overall score above 50 indicates a high scouring potential.

The PIEF is an efficient and economic approach to determine the scour potential at bridge sites. However, the evaluated items, the number of levels and the weights (β and α) are mainly determined by the experts' judgments. In this case, the PIEF is often subjective and lacks concrete evidence. Because uncertainties in the evaluated items are inevitable, a probabilistic approach is adopted to establish a reliability-based PIEF. This study uses a Bayesian network (BN) to perform a scour reliability analysis. The proposed BN consists of two parts. The first part evaluates the scour potential and is established mainly on the basis of the PIEF developed by China Engineering Consultants, Inc. The second part calculates the scour reliability, which is first evaluated by stability analysis and then updated via a Bayesian approach with the historical records at the bridge sites. The 13 items identified in Table 1 are chosen to be the factors that impact the scour potential at bridge sites. In addition, the weights (β and α) in Table 1 are used to build the conditional probability table (CPT) of the proposed BN. This CPT is used to determine whether the inspected bridge has a low, medium or high scour potential. The proposed PIEF is built by establishing a close correlation between the PIEF and BN reliability by revising the weights (α) used in Table 1. Thus, the probabilistic characteristics in the scour potential are implicitly considered in the proposed PIEF. The analysis flowchart of this study is illustrated in Figure 2.

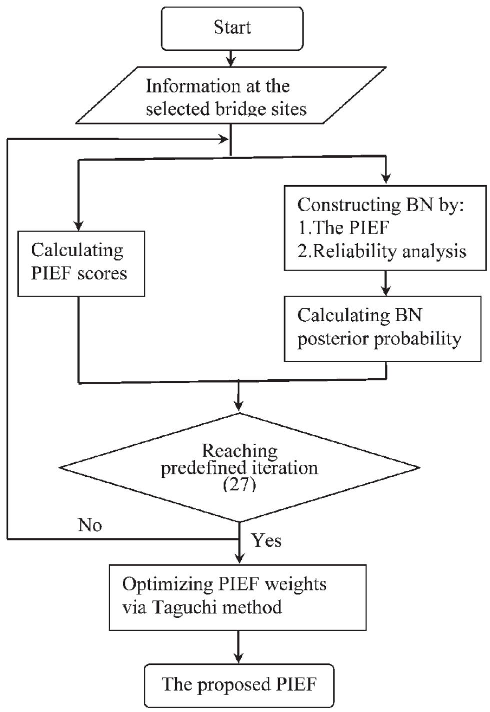

Fig. 2. The flowchart of this study

To demonstrate the details of the proposed algorithm, a reliability-based PIEF is constructed for bridges on the Gaoping River Basin of Taiwan. The Gaoping River Basin has numerous bridges and many tributaries, including the Qishan River, the Laonong River, the Meinong River and the Chuokou River. This study examines 32 bridge sites that were seriously impacted by Typhoon Morakot (Fig. 3). To capture the uncertainty characteristics at different locations on the Gaoping River Basin, 15 of the 32 sites that had sufficient recorded data are selected for reliability analysis; these sites are shown in Figure 3. For example, the variations in hydraulic characteristics (e.g., water level and stream velocity) are used to calculate the reliability at these 15 sites. In addition, this study only focuses on bridges with pile foundations; thus, pile foundations are assumed to be present in the bridges at the selected 15 sites, though the bridges may have other foundation types. In other words, the bridges analyzed here are not necessarily the actual bridges on the Gaoping River Basin. Nevertheless, we believe that variability of bridges with pile foundations in this area is fully described by the random variables at these 15 sites.

Because the bridges analyzed here may not be the actual bridges present, the bridge sites are numbered to avoid confusion. For example, the bridge at the Yuemei Bridge site is called Bridge No. 13 (Table 2). Similar abbreviations used for other bridges are shown in Table 2.

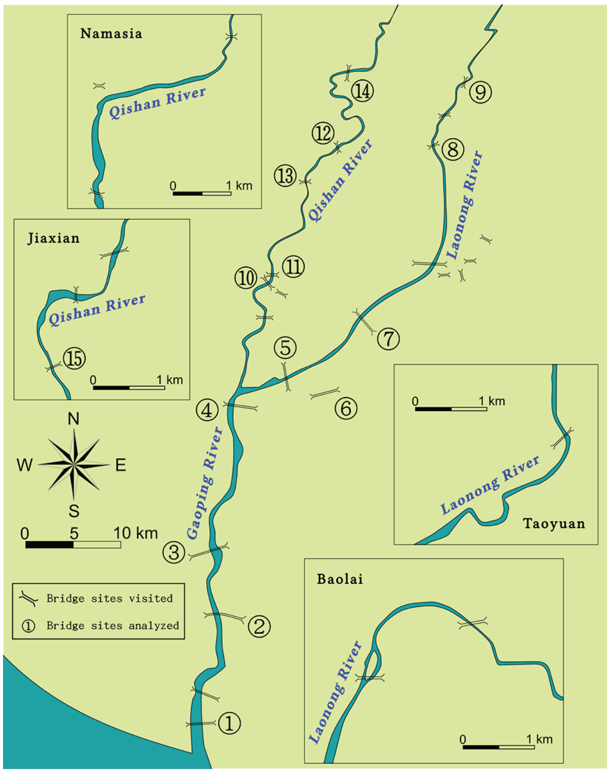

Fig. 3. Bridge sites for in-situ survey (denoted as a bridge figure) and reliability analysis (denoted as a number) on the Gaoping River Basin

Although a probabilistic method is used to evaluate the scour potential at the bridge sites, the results are converted into a PIEF, which is popularly used by practicing engineers. Thus, the research results can be implemented with existing evaluation procedures in Taiwan.

1. Uncertainties considered in this study

The random variables considered in this study include water level, stream velocity, local scour depth, live load, dead load and the geometric sizes of bridges (i.e., pile length, pile diameter, pier height and pier diameter). The statistical information for all the random variables except pile length is described in Tables 2–5. Note that the geometric sizes are considered as random variables only if there is no design drawing or other information for the evaluated sites. Measurements of pile diameter, pier height and pier diameter were collected from the design drawings or in-situ measurements. Because the collected samples are limited, they are simulated as a uniform distribution, in which the maximum and minimum values of the samples are regarded as the upper and lower bounds of the distribution. The design live load and the wind load are calculated based on the "The Bridge Design Specifications" (Ministry of Transportation and Communications 2009). Because the magnitudes of the live load and the wind load depend on the span and pier height, respectively, their variability is described by a uniform distribution. The detailed statistical properties for water level, stream velocity, local scour depth and pile length are described below.

Table 2. Bridge abbreviation and statistical parameters (unit: meter) for water level*

Bridge name	Representative name	μ**	*cov****
Shuangyuan bridge	No. 1 bridge	10.50	
Wanda bridge	No. 2 bridge	9.52	
Kaoping bridge	No. 3 bridge	9.55	
Liling bridge	No. 4 bridge	8.83	
Ligang bridge	No. 5 bridge	7.56	
Kaoshu bridge	No. 6 bridge	10.56	
Kaomei bridge	No. 7 bridge	10.92	
Liouguei bridge	No. 8 bridge	8.90	0.13–0.14
Xingfa bridge	No. 9 bridge	8.05	
New Qiwei bridge	No. 10 bridge	10.63	
Qishan bridge	No. 11 bridge	9.73	
Shanlin bridge	No. 12 bridge	8.94	
Yuemei bridge	No. 13 bridge	6.86	
Baolong bridge	No. 14 bridge	9.93	
Chiahsien bridge	No. 15 bridge	7.67	

*Log-normal distribution; **mean value; ***coefficient of variation.

Table 3. Stream velocity* statistical parameters (unit: meter/second)

Bridge name	μ	*cov*
No. 1 bridge	3.38	0.3–0.4
No. 2 bridge	3.03	
No. 3 bridge	3.05	
No. 4 bridge	3.63	
No. 5 bridge	3.04	
No. 6 bridge	4.83	
No. 7 bridge	1.99	
No. 8 bridge	4.80	
No. 9 bridge	5.10	
No. 10 bridge	3.34	
No. 11 bridge	4.04	
No. 12 bridge	6.49	
No. 13 bridge	4.39	
No. 14 bridge	3.07	
No. 15 bridge	3.83	

*Log-normal distribution.

1.1. Water level and stream velocity

The design values of a 100-year flood specified in the "The Bridge Design Specifications" (Ministry of Transportation and Communications 2009) are used as the mean values of water level and stream velocity. Their distribution types and variations are explained as follows. Based on the previous studies as shown in Table 6 (Johnson 1992, 1995, 1996, 1999; Yanmaz 2003; Johnson, Dock 1998; Ghosn, Wang 2003; Cesare 1991; Mays, Tung 1992; Yeh, Tung 1993; Tung 1990), the covs of water level and stream velocity fluctuate among studies. For example, the cov of water level varies from 0.2 to 1.09. Table 6 also indicates that a single distribution cannot universally describe hydraulic parameters for all cases. Because variations/distributions of hydraulic parameters often depend on its region/location, it may not be a good strategy to adopt the variations/distribution used in the literature. Thus, to reveal the variations/distributions of water level and stream velocity on Gaoping River Basin, a probabilistic hydraulic analysis using HEC-RAS (Hydrologic engineering center-river analysis system, Army Corps of Engineers, Hydrologic Engineering Center 1997) with random variables of discharge rate and Manning's roughness coefficient is performed.

The water level and stream velocity simulated by HEC-RAS are then plotted on 6 probability plots to identify their distribution as shown in Figure 4 (for the case of water level). It is found that the Log-normal is the most suitable distribution for both parameters. The chi-square goodness of fit test is used to determine whether simulated sample data (i.e., water level and stream velocity) are consistent with the hypothesized distribution (i.e., Log-normal distribution). Comparing the p-values (0.973 and 0.5658 for water level and stream velocity, respectively) to the usual significance level (5%), the null hypothesis cannot be rejected at the 5% significance level. Thus, the Log-normal distribution is appropriate to describe the water level and stream velocity.

In addition, from the simulation of HEC-RAS, the covs of water level at different bridge sites range from 0.13 to 0.14. The covs of stream velocity at different bridge sites range from 0.3 to 0.4. Because above observations rely on the collected data (i.e., Manning's roughness coefficient and discharge rate, details are explained

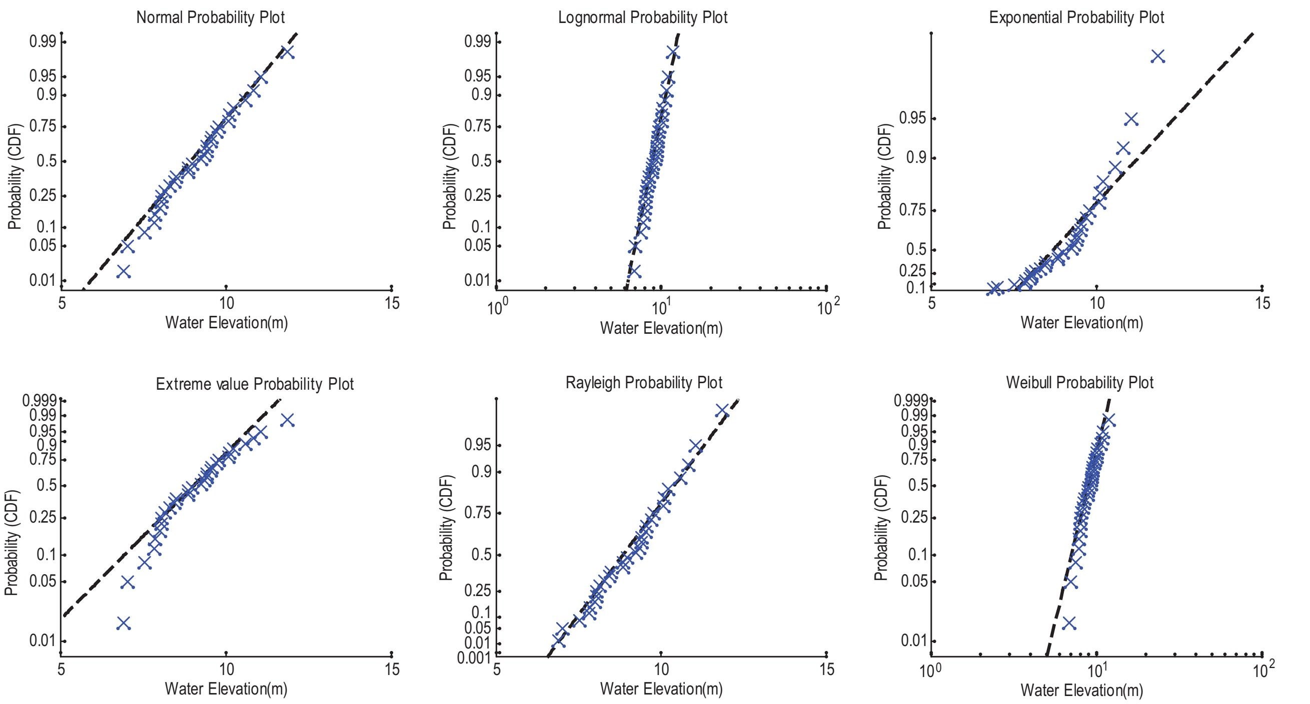

Fig. 4. Probability plots for the water level at No.1 bridge site

in the next paragraph), different data may result in a slightly different outcome. To capture this uncertainty, the cov of water level/stream velocity is simulated as a uniform random variable with ranges described above in the stability-based reliability analysis (Tables 2 and 3).

It is known that Manning's roughness coefficient and discharge rate are two of the major factors that affect the outcomes of HEC-RAS. For the Gaoping River Basin, Manning's roughness coefficient can be modeled as lnN(–3.395, 5.508), lnN(–3.571, 0.575) and lnN(–3.802, 0.664) for the upstream, midstream and downstream, respectively (Wu *et al.* 2001). Sheen (2012) indicated that discharge rate can be modeled as $N(Q_{100}, 0.18^2)$. The above data are adopted here to generate random number for the input of HEC-RAS. The HEC-RAS model built here is verified by the water level and stream velocity at the nearest cross section to the seashore reported in the government document (Ministry of Economic Affairs 2008). Due to the input factors, cross sections and hydraulic analysis model used here may be different from those used in official calculation, it is expected that hydraulic parameters (water level and stream velocity) calculated in this study will deviate from that of the government report. The difference percentage is controlled to be less than 5% to ensure the accuracy of the built model. A simulated water level and three cross sections (i.e., No. 1, 2 and 3 bridge sites) for Gaoping River are illustrated in Figure 5.

1.2. Local scour depth

Local scour depth can be calculated using an empirical formula. Recent studies have proposed many formulae for calculating local scour depth. Li *et al.* (2011) proposed seven suitable formulae for use in Taiwan. Of these seven formulae, five are used to compute the local scour depth (i.e., Neill 1965; Shen *et al.* 1966, 1969; Jain, Fischer 1980; Jain 1981). Because above formulae are not up-to-date, two additional formulae are added to improve the prediction accuracy (Fischenich, Landers 1999; U.S. Department of Transportation 2012). For the latter two formulae, two cases for the attack angle of flow (0^0 and 30^0) are considered. Figure 6 illustrates the

Table 4. Local scour depth* statistical parameters (unit: meter)

Bridge Name	μ	σ**
No. 1 bridge	9.73	2.74
No. 2 bridge	8.07	2.23
No. 3 bridge	6.43	1.66
No. 4 bridge	7.54	2.02
No. 5 bridge	8.63	2.40
No. 6 bridge	8.27	2.19
No. 7 bridge	8.45	2.40
No. 8 bridge	7.16	1.79
No. 9 bridge	7.40	1.86
No. 10 bridge	9.30	2.58
No. 11 bridge	8.62	2.36
No. 12 bridge	7.63	1.96
No. 13 bridge	6.27	1.57
No. 14 bridge	7.36	1.95
No. 15 bridge	8.14	2.19

*Log-normal distribution; ** standard deviation.

Table 5. Statistical parameters of pile diameter, pier height, live load and wind load*

Random Parameter	Max. Value	Min. Value
Pile diameter	0.9**	0.4
Pier Height	Water Level +2.4**	Water Level +1.8
Pier diameter	4.2**	1.8
Live Load	155***	115
Wind Load	18***	14

*Uniform distribution; **unit: meter; ***unit: ton.

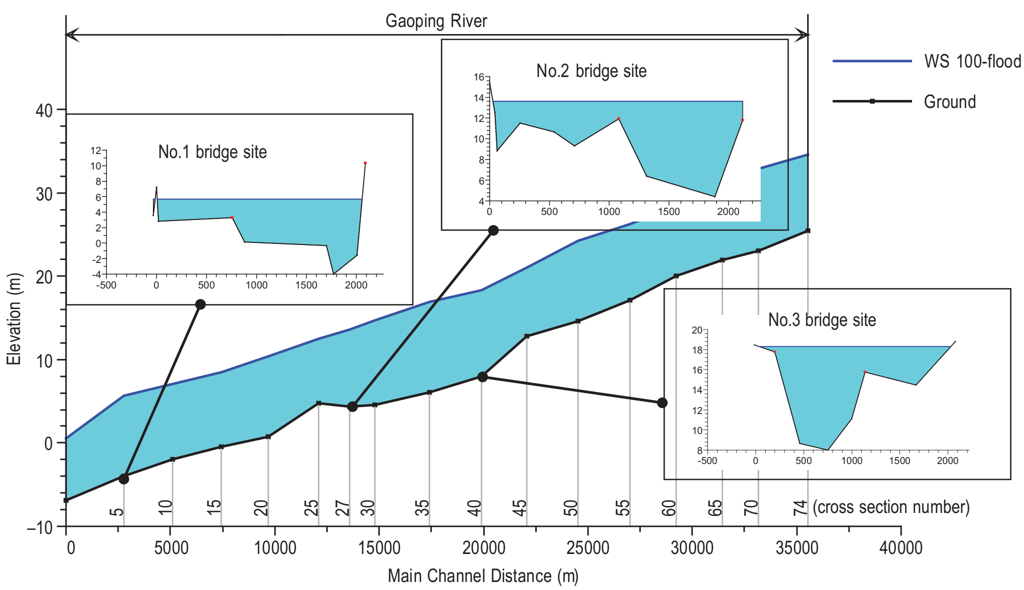

Fig. 5. Water surface profile and three cross sections on the Gaoping River

Table 6. covs and distributions of hydraulic parameters used in literatures

variable	cov	distribution	Location/reference
Water level	0.2	Symmetrical triangular	Piney Creek/1
Water level	0.2	Symmetrical triangular	South Fork Forked Deer River/1
Water level	0.23	normal	laboratory data/3
Water level	1.09	NA	Collected field data/4
Jet flow velocity	0.2	Symmetrical triangular	Outlet facilities/2
Stream velocity	0.2	Symmetrical triangular	South Fork Forked Deer River/1
Stream velocity	0.329	NA	laboratory data/3
Stream velocity	0.51	NA	Collected field data/4
Stream velocity	$0.008x^a$	triangular	NA /11
Stream velocity	$0.012x^b$	uniform	NA /11
Stream velocity	0.2	Symmetrical triangular	Piney Creek/1
Stream velocity	0.04	Symmetrical triangular	Bonner bridge/5
Scour depth	0.357	NA	laboratory data/3
Scour depth	0.85	NA	Collected field data/4
Scour depth	0.03	Symmetrical triangular	Bonner bridge/5
Manning roughness	0.28	Log-normal	Schoharie river *et al.*/6
Manning roughness	0.1, 0.15	normal	NA/7
Manning roughness	0.2, 0.053	normal	NA /8
Manning roughness	0.08	triangular	NA /9
Manning roughness	0.1, 0.055	Triangular, gamma	NA./10
Manning roughness	0.2-0.35	Log-normal	NA /11
Manning roughness	0.28, 0.18	uniform	NA /11
Manning roughness	NA	uniform	NA/3
Discharge rate	0.21-0.25	Log-normal	Schoharie river *et al.*/6

1 Johnson (1999); 2 Yanmaz (2003); 3 Johnson (1992); 4 Johnson (1995); 5 Johnson and Dock (1998); 6 Ghosn and Wang (2003); 7 Cesare (1991); 8 Mays and Tung (1992); 9 Yeh and Tung (1993); 10 Tung (1990); 11 Johnson (1996).

results of local scour depth at Bridge No. 10. The formula proposed by Neill (1965) results in the maximum local scour depth, while the HEC-18 (U.S. Department of Transportation 2012) without attack angle gives the minimum local scour depth. Note that water level and stream velocity are random variables. Figure 6 only displays the mean value for each formula. Based on 6 probability plots (Fig. 7) and the chi-square goodness of fit test, it is confirmed that the Log-normal distribution is suitable to describe the local scour depth at a bridge site (e.g., the p-value is 0.4116).

Mean value of the scour depth is the sample mean and the standard deviation is one-sixth of the difference between the maximum and minimum depths. Please note that this assumption indicates that the actual scour depth has probability of 99.73% located within the range calculated by these seven empirical formulae. The total scour depth of the pier is generally the sum of the depths of local scouring, contraction scouring, movable riverbed and long-term scouring. The contraction scour depth and the long-term scour depth were implicitly considered in the first part of the BN in this study (items 3 and 4, respectively). In addition, the movable riverbed is comparatively small and thus is not considered at present.

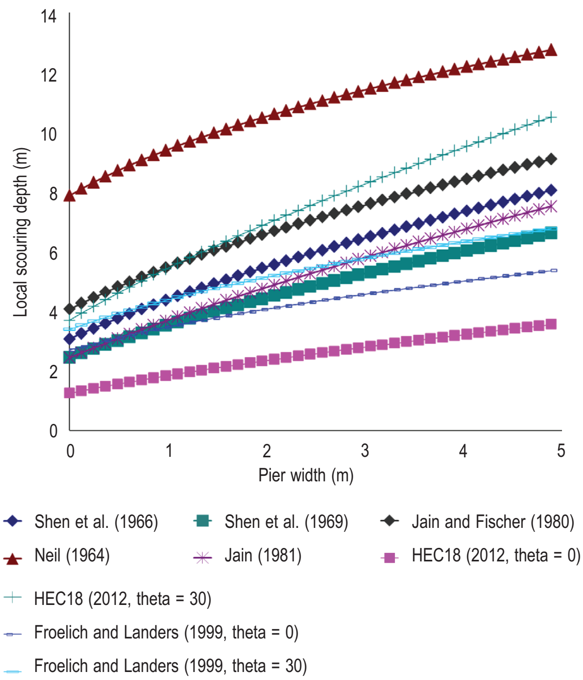

Fig. 6. Results of local scour depth using empirical formulae at No. 10 bridge site

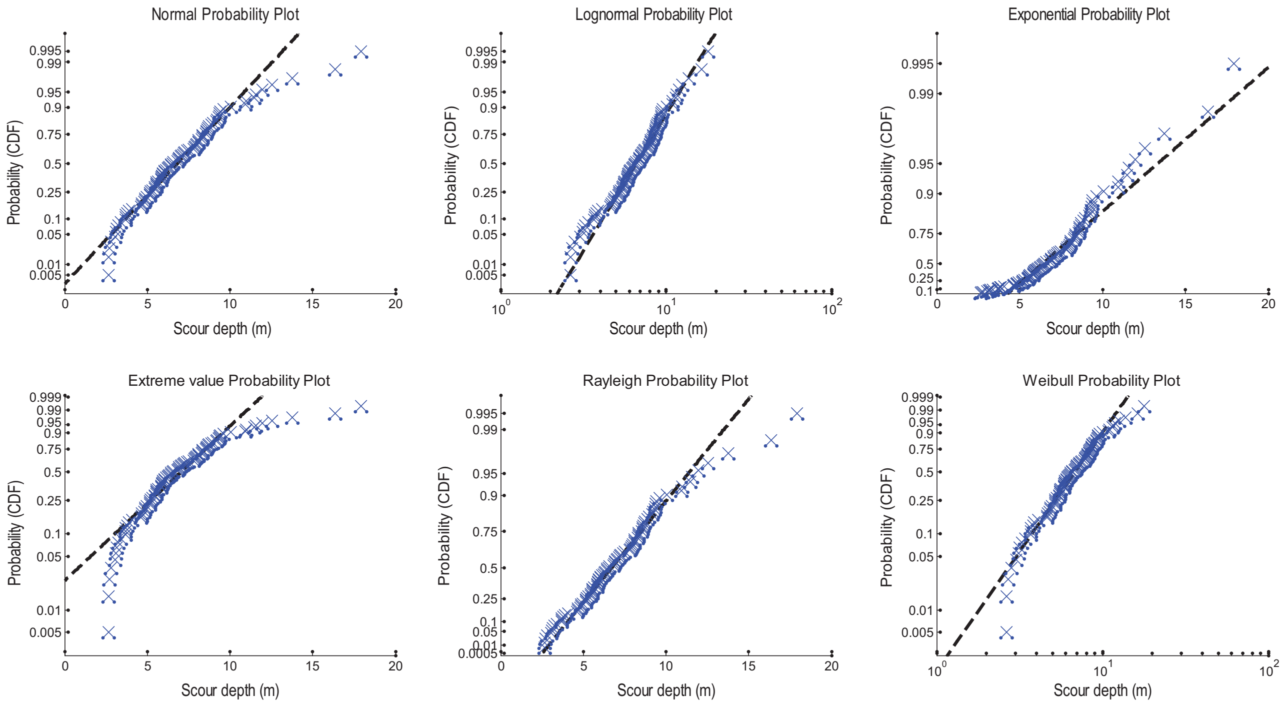

Fig. 7. Probability plots for the scour depth at No. 10 bridge site

1.3. Pile length

According to Wang (2002), the soil conditions and bridge foundations of the Gaoping River Basin can be approximately described as follows:

– A. The standard penetration test value (SPT-N) in the first 20 m of soil is a constant value in each 5 m depth interval;
– B. The SPT-N between 20 m and 40 m depth is a constant value in each 10 m depth interval;
– C. The maximum pile length is 40 m.

Based on the conditions described above, there are six soil layers, and the soil layers are numbered down from the surface. For example, the first soil layer extends from the ground surface to 5 m below ground level. The pile lengths are categorized into four types described below:

1. If the SPT-N value of the first soil layer is greater than 50, the pile length follows a uniform distribution with upper and lower bounds of 20 m and 2 m, respectively (type I).
2. If the sum of the SPT-N values of the first and second soil layers is greater than 50, the pile length follows a uniform distribution with upper and lower bounds of 20 m and 10 m, respectively (type II).
3. If the sum of the SPT-N values from the first four layers is greater than 50, the pile length follows a uniform distribution with upper and lower bounds of 40 m and 15 m, respectively (type III).
4. In other cases, the pile length follows a uniform distribution with upper and lower bounds of 40 m and 20 m, respectively (type IV).

As mentioned above, the pile length is determined by the SPT-N value of the bridge site. Because the Central Geological Survey of the Ministry of Economic Affairs (MOEA) in Taiwan does not have drilling data from all the bridge sites, the SPT-N value of the bridge site was estimated using the ordinary kriging method as described below.

An experimental variogram was first constructed by calculating the variance of each drilling point in the set with respect to each of the other points. Using this variogram with the performance index (R-square, R^2) and the sequential quadratic programming (SQP) technique, an adequate mathematical model with suitable threshold and effective range was then found. Third, the mathematical model selected in the second step was applied to compute the weights (λ_i) used in the ordinary kriging model, as shown in Eqn (1):

$$\hat{Z}(x_0) = \sum_{i=1}^{n} \lambda_i Z(x_i), \tag{1}$$

where $\hat{Z}(x_0)$ is the kriging estimate at the non-sampled location x_0, $Z(x_i)$ is the value sampled at location x_i, λ_I is the weighting factor for $Z(x_i)$ and n is the number of points in the set. There were 25 existing borehole locations on the Gaoping River Basin as shown in Figure 8.

The experimental variogram of N_2 (the second layer) is shown in Figure 9, in which h is the distance (meter) between two points and is calculated based on the TWD67 coordinate system, $r(h)$ represents semi-variance and is computed by Eqn (2):

$$\gamma(h) = \frac{\sum_{i=1}^{N} \left[z(i) - z(i+h) \right]^2}{2N}, \tag{2}$$

where N is the set of location pairs, $z(i)$ is the i^{th} variable under consideration as a function of the location of

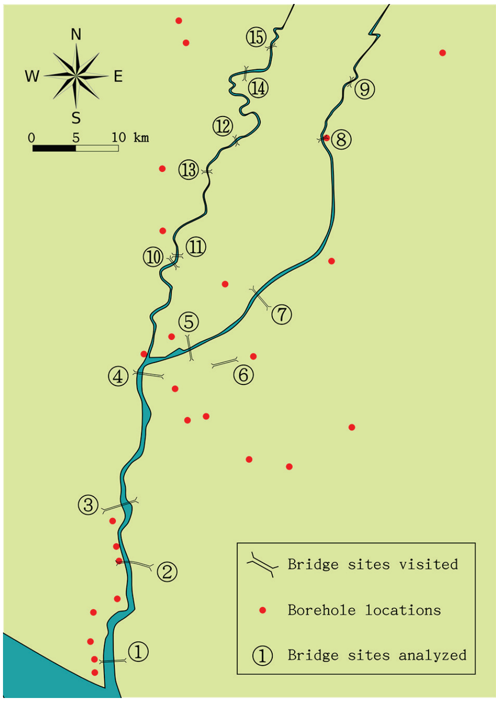

Fig. 8. Locations of the 25 borehole locations (denoted as a red dot) and 15 bridge sites on the Gaoping River Basin

i (i.e., the SPT-N value), $z(i+h)$ is the SPT-N value with distance of h from the location of i.

Based on Figure 9, a Gaussian model was used for the kriging estimation. Moreover, the SPT-N values of the layers were estimated independently without mutual influence. The estimated results of the SPT-N values of various soil layers are shown in Table 7. The effective ranges, thresholds and corresponding R^2 values of soil layers are shown in Table 8. Except the first layer (N_1), the R^2 for each layer was greater than 0.8.

Table 7. Coordinates and estimated SPT-N values at the 15 bridge sites

Bridge	X	Y	N_1	N_2	N_3	N_4	N_5	N_6
No. 1	187757	2487657	13	15	17	18	18	24
No. 2	187719	2489106	11	14	13	18	34	40
No. 3	187297	2490927	8	17	13	23	42	48
No. 4	187609	2494008	20	45	37	52	68	68
No. 5	190480	2499455	42	62	59	68	78	76
No. 6	190130	2495436	56	66	67	72	80	77
No. 7	204047	2510144	77	87	90	90	92	87
No. 8	208288	2509379	100	100	100	100	100	100
No. 9	214896	2513530	100	99	93	99	100	100
No. 10	189637	2503648	47	80	79	84	88	85
No. 11	196232	2517596	31	74	71	79	85	82
No. 12	212754	2531063	79	100	100	100	100	100
No. 13	204497	2521006	69	100	100	100	99	96
No. 14	193191	2521342	81	100	100	100	100	100
No. 15	195863	2523092	85	100	97	100	100	100

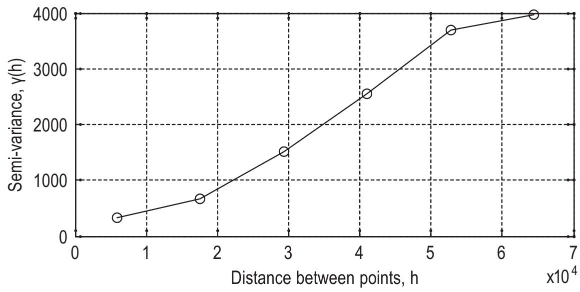

Fig. 9. The experimental variogram for N_2

Table 8. Effective range, threshold and R-square of various soil layers

Parameter	Threshold		Effective range	R-square
	C_0	C_1	a	R^2
N_1	184.24	1971.61	45563.64	0.74
N_2	366.68	888.21	34043.86	0.84
N_3	321.13	1174.61	32564.99	0.87
N_4	287.48	1617.36	29571.67	0.85
N_5	278.85	663.58	33890.99	0.87
N_6	289.11	940.98	46126.17	0.81

2. The construction of the BN

A BN is used to calculate bridge scour reliability in this study. The reasons for adopting a BN are described below:

(1) Many factors affect bridge scour reliability. The BN breaks down these various factors and makes them as nodes in the network, allowing one to focus on the causal relationship between two nodes at each time. Thus, the problem's complexity is reduced.

(2) The BN allows users to update the scour reliability through Bayesian learning. The availability of current data for evaluating a bridge scour problem is often limited. In addition, data from future floods should contribute to the scour reliability calculations. Thus, an evaluation process with learning capability is needed.

(3) For a problem with incomplete data, the BN can utilize expert opinions to determine the conditional probability between nodes to facilitate the reliability analysis.

The first step in constructing the proposed BN is to establish the network topology that reflects causal relationships of various nodes. The second step is to establish the conditional probability between the nodes, and the third step is to update the parameters using the Bayesian theorem. Based on the existing PIEF, this study used the AgenaRisk software (Agena Ltd. 2007) to establish the proposed BN and its topology is shown in Figure 10. AgenaRisk (Agena Ltd. 2007) is a graphical user interface (GUI) tool for modeling risk and for making predictions about uncertain events in a wide variety of problems. AgenaRisk (Agena Ltd. 2007) provides a spreadsheet-based analysis in which BN and statistical simulation such as Markov Chain Monte Carlo Simulation (MCMC) are integrated. In addition, AgenaRisk

(Agena Ltd. 2007) supports both diagnostic and predictive reasoning about uncertainty.

The network construction principles are described below.

2.1. The topology of the proposed BN

The network is composed of two parts as shown in Figure 10. The first part is the top left area above the red dashed line, and the second part is the rest of the BN. The first part is illustrated as follows. The PIEF (Table 1) has 13 assessment items; they are divided into four potential factors by cause of scouring, including: (1) eroded river bed; (2) river bank erosion; (3) area ratio of bridge to cross section; and (4) foundation exposure depth. These four factors are served as the parent nodes of the scouring potential node. The second part of the network provides two additional conditional probabilities, which are the probabilities of bridge failure given that there is or is not scour potential. As mentioned above, the two conditional probabilities are obtained by reliability analysis; details are explained in Section 3.

According to the descriptions and Figure 10, the eroded river bed node consists of four parent nodes, including upstream dam or reservoir facilities, material on the river bed, hydraulic drop effect and protection for the river bed. River bank erosion has three parent nodes, including bending or narrowing of the river, location of the main channel and protection for the river bank. The area ratio of bridge to cross section has two parent nodes, including the bending or narrowing of the river and the effective pier diameter. The foundation exposure depth has four parent nodes, including upstream dam or reservoir facilities, hydraulic drop effect, foundation type and flow angle. The node of bridge failure probability has only one parent node that is scouring potential. The historical scouring data is the only child node for bridge failure probability node.

The advantages of establishing the network topology on the basis of the existing PIEF are as follows: (1) given the numerous potential factors that affect scouring, building the network on the basis of the existing 13 items, which are screened by experts, can maintain a reasonable BN dimension to avoid computational burdens; (2) the conditional probability can refer to the allocated weights of the existing PIEF as described in Section 2.2.

2.2. Conditional probability in the network

2.2.1. Conditional probability in the first part of the BN

Conditional probability is needed for six nodes, including eroded river bed, river bank erosion, area ratio of bridge to cross section, foundation exposure depth, potential of scouring and bridge of failure probability. Because a similar rule is applied to each of the first five nodes, a detailed explanation is only provided for the node of the eroded river bed. The conditional probability for bridge of failure probability node is described in Section 2.2.2.

The node of the eroded river bed (assuming two levels) consists of four parent nodes, including protection for the river bed (four levels, Table 1), hydraulic drop effect (assuming two levels), upstream dam or reservoir facilities (three levels, Table 1) and material on the river bed (five levels, Table 1). The weights (α) of these four nodes in Table 1 are 10, 5, 7 and 2, respectively. The weight proportions of each parent node are calculated using Eqn (3):

$$w_i = \frac{b_i}{\sum_{i=1}^{4} b_i}, \tag{3}$$

where w_i is the weight proportion of node i (i indicates the parent node) and b_i is the weight (α) of node i. Because the node of hydraulic drop effect is considered to impact the nodes of both the eroded river bed and the foundation exposure depth, b_i of the hydraulic drop effect node at the eroded river bed is only half of its weight (α). For example, the hydraulic drop effect node's b_i value is 5/2 = 2.5.

Based on the level number of each parent node, the node of the eroded river bed has 120 different conditions (4 × 2 × 3 × 5 = 120). For each condition, the probabilities of having or not having an eroded river bed must be

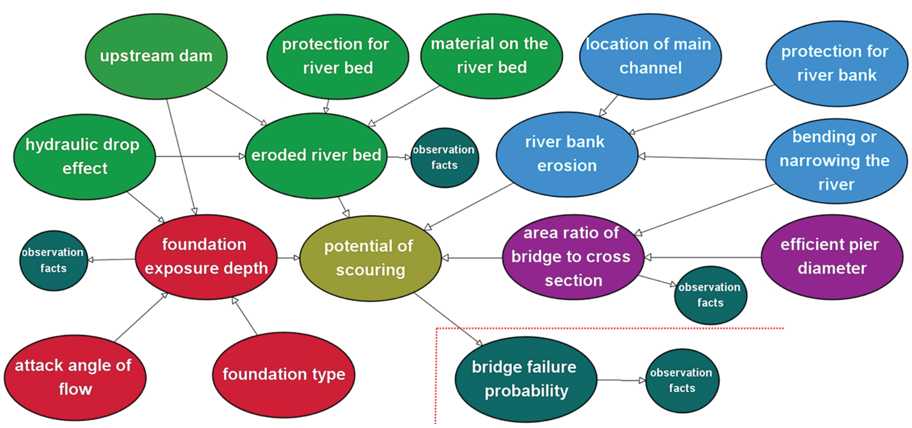

Fig. 10. Bayesian network used in this study

determined; that is, 240 conditional probabilities need to be defined. In addition, the sum of the two probabilities at each condition must be equal to one. In this study, a normal distribution with lower and upper bounds of 0 and 1 is used to describe the probability behavior for each condition (e.g., 120 normal distributions are used at the current node being considered). The mean value (μ_j) of each normal distribution is calculated using Eqn (4):

$$\mu_j = \sum_{i=1}^{n} w_i X_i, \tag{4}$$

where w_i is the weight proportion of node i (i indicates the parent node), X_i is the index value for the i^{th} parent node, n is the number of parent nodes, j is the j^{th} condition and X_i is determined by the following rules:

1. X_i value ranges between 0.0 and 1.0.
2. If the parent node has two levels, the X_i value of the first level is 1.0, and the X_i value of the second level is 0.0; if the parent node has three levels, the X_i values for each level are 1.0, 0.5 and 0.0, respectively. Similar rules are applied to other situations.

The conditional probability is calculated as described below:

1. The standard deviations of the normal distribution are arbitrarily selected.
2. With the normal distribution, if the child node (e.g., eroded river bed) has two levels, the probabilities of the first and second levels at each condition are the cumulative probabilities with ranges from 0 to 0.5 and from 0.5 to 1.0, respectively. Similar rules are applied if the child node has more than two levels.

The conditional probability is affected by the selected standard deviation. Taking a BN with three nodes as an example (Fig. 11), because each node has two levels, there are eight conditional probabilities (probabilities (a)–(h) in Fig. 11). The mean value of the normal distribution for probability (a) and (e) is calculated as follows (assuming the standard deviation is 0.0):

$$u_1 = 0.5\times1 + 0.5\times1 = 1;$$
$$\sigma = 0.0. \tag{5}$$

Based on the definition described above, the probabilities of (a) and (e) are 1.0 and 0.0, respectively. Both parent nodes have the same tendency to result in a level 1 in their child nodes. This is true for the existing PIEF (Table 1). It should be noted that the effects of the parent nodes on the child nodes are not necessarily the same.

	Node A	
	level 1	level 2
Probability	0.6	0.4

	Node B	
	level 1	level 2
Probability	0.3	0.7

w_a = 0.5 w_b = 0.5

		A = level 1		A = level 2	
		B = level 1	B = level 2	B = level 1	B = level 2
Probability	C = level 1	(a) = 1.0	(b) = 0.5	(c) = 0.5	(d) = 0.0
	C = level 2	(e) = 0.0	(f) = 0.5	(g) = 0.5	(h) = 1.0

Fig. 11. A three-node BN (σ = 0)

Another extreme case is for $\sigma = \infty$. Although u_1 in Eqn (5) remains the same, the probabilities of (a) and (e) now are 0.5 and 0.5, respectively. In this case, no apparent relationship between parent and child nodes can be identified. This conclusion remains the same if X_i is described as follows (σ = 0).

If the parent node has two levels, the first level's value of X_i is 0.5, and the second level's value of X_i value is 0.5.

That is, in the case where the analyst cannot determine the impact of the parents' levels on the child node, one can either increase the standard deviation or reduce the difference between the X_i values in the different levels. In addition, Eqn (4) shows that the mean value (μ) is determined by w_i and X_i. The value of w_i is calculated on the basis of the α values in Table 1. For most cases, the value of X_i is same as that of β in Table 1. Thus, the conditional probabilities of the first part of the BN are established mainly on the basis of the existing PIEF.

2.2.2. The conditional probabilities of the second part of the BN

The existing PIEF does not contain the second part of the BN. The conditional probabilities of this part are calculated under two cases: with or without scouring potential. If there is no scouring potential, we assume the current scour depth to be 0.0 and compute the probability of failure. If there is scouring potential, we assume that the scour depth is random (Section 1) and calculate the probability of failure probability using a stability analysis.

2.3. Updating of the BN

To further reflect the local characteristics of each bridge site, the Bayesian theorem is used to update the probability of failure. When a bridge is damaged, a new bridge is often rebuilt near the original site due to limitations of the urban environment and traffic routes. Though the new bridge structure may differ from the previous bridge, the river conditions are similar. Therefore, the historical damage record of a bridge site can be used as a reference.

This study assumes that the failure probability is a constant number for a given bridge site. Therefore, failure occurrence should follow a binominal distribution. Because the failure probability is often not known, it is assumed to be a beta random variable between 0.0 and 1.0. Based on observations (e.g., the historic scouring data at the considered node), the posterior failure density function ($f''(\theta)$) can be calculated using Eqn (6):

$$f''(\theta) = \frac{P(\varepsilon\,|\,\theta)f'(\theta)}{\int_{-\infty}^{\infty} P(\varepsilon\,|\,\theta)f'(\theta)d\theta}, \tag{6}$$

where $f'(\theta)$ is the prior failure density function; in which θ are distribution parameters such as the shape parameters in beta distribution. These shape parameters are calculated by assuming that the mean value is the failure probability from stability-based reliability analysis and the cov is 0.05. ε is the number of times that failure was observed in a specified period (T). Table 9 displays the flood return period of the recorded scouring event for each bridge site. Based on this observation, ε and T are taken as one and the flood return period in Table 9, respectively. $T = 300$ indicates that there is no recorded scouring event at that site. In addition, this study uses the mean value of $f''(\theta)$ as the posterior failure probability.

Table 9. Flood return period (T) of the recorded scouring event at 15 bridge sites

Bridge	1	2	3	4	5	6	7	8	9	10	11	12	13	14	15
T	100	300	200	200	50	200	200	100	100	100	100	100	300	300	50

3. Reliability analysis

Five limit state functions are considered in the stability-based reliability analysis. According to the "The Bridge Design Specifications" (Ministry of Transportation and Communications 2009), the limit state function of the supporting force is:

$$A_s f_s + A_b q_b - \frac{P}{n \times m} - \sigma A = 0, \qquad (7)$$

where: A_s is the pile surface area, f_s is the friction resistance force on the surface of the pile, A_b is the area of the pile bottom, q_b is the allowable vertical force at the pile bottom, P is the applied vertical load, $n \times m$ is the total number of piles, σ is the resulting stress of the outermost pile due to the bending moment, and A is the pile area. The limit state function of the soil pulling force is:

$$w_p + A_s f_s + \frac{P}{n \times m} - \sigma A = 0, \qquad (8)$$

where w_p is the pile weight. According to Chang and Chou (1989), the limit state function of the pile shear stress (Eqn (9)), the pile axial stress (Eqn (10)) and the horizontal displacement on the top of pile (Eqn (11)) are described as follows:

$$A\tau_y - V_t e^{-\lambda x}[\cos(\lambda x) - (1 + 2\lambda h_0)\sin(\lambda x)] = 0; \qquad (9)$$

$$\frac{I\sigma_y}{y} - \frac{V_t}{\lambda} e^{-\lambda x}[\lambda h_0 \cos(\lambda x) + (1 + \lambda h_0)\sin(\lambda x)] = 0; \qquad (10)$$

$$1.5 - 0.01\left(\frac{H}{2EI\lambda^3} + \frac{M_t}{2EI\lambda^2}\right) = 0, \qquad (11)$$

where: τ_y is the allowable shear stress of the pile, V_t is the applied shear force on the top of the pile (tf), $\lambda = \sqrt[4]{kD/EI}$ (m^{-1}), k is the horizontal subgrade reaction coefficient (tf/m^3), D is the pile diameter (m), E is the elastic modulus (tf/m^2), I is the pile cross sectional moment of inertia (m^4), σ_y is the allowable axial stress, y is the distance of the outermost point to the neutral axis, $h_0 = M_t/V_t$ (m), M_t is the applied bending moment on the top of the pile (tf–m) and H is the force acted on pile due to water pressure (tf). The stability-based reliability analysis is conducted using Monte Carlo simulation (MCS) with a sample size of 10^4. A series system is assumed in this study; that is, a component failure will result in a system failure.

Figure 12 illustrates the results for the site of Bridge No. 13. The long red bars represent demand, and the long blue bars or lines denote capacity. Because the material uncertainty is not considered, the capacities of

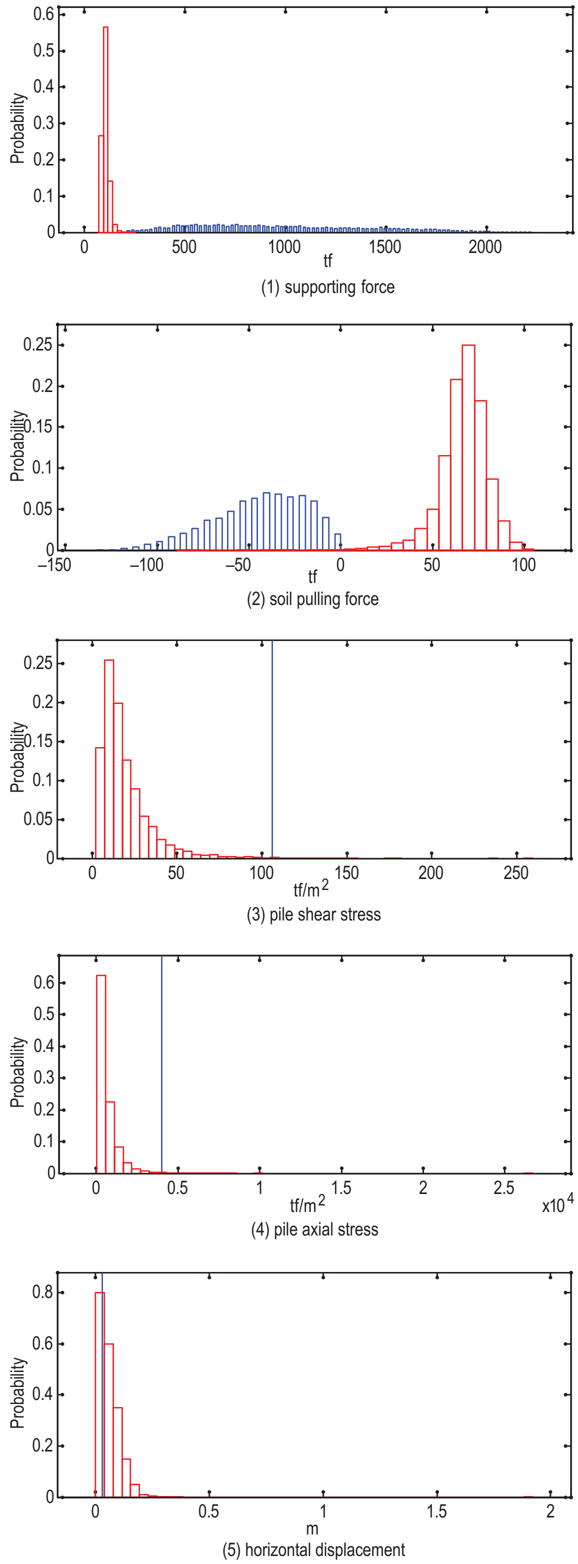

Fig. 12. Results of reliability analysis (Bridge No. 13)

the shear stress and the axial stress are constant. In addition, the displacement capacity is a constant provided by the specifications (1.5 cm as indicated in Eqn (11)). As shown in Figure 12, the displacement requirement dominates the system reliability. Table 10 illustrates the failure probabilities at 15 bridge sites. Note that number of simulation cycles will influence the level of reliability in MCS. Therefore, simulations should be carried out several times for large cycles such that the corresponding value of C_r (i.e., cov) is relatively small (Melchers 2002). C_r can be calculated by the Eqn (12) displayed below (Naess *et al.* 2009; Ang, Tang 1984):

$$C_r(p_f) = \sqrt{\frac{1-p_f}{p_f N}}, \tag{12}$$

where P_f is the estimated system failure probability and N is the sample size. Because only the failure probability with scouring potential has an influence on the BN analysis, the corresponding C_r is provided for each bridge site as shown in Table 10. It is found that none of C_r is larger than 10%. Thus, the sample size of 10^4 is adequate (Johnson 1999).

In addition to the consideration of sample size, to verify the probability calculated by MCS, the reliability of bridge No. 8 is evaluated by both MCS and first order reliability method (FORM). Table 11 displays failure probabilities obtained from FORM and MCS. Please note that for a system reliability problem, FORM is often associated with a bounding technique to deliver a failure probability. Although several bounding techniques have been proposed (Zhao *et al.* 2007), investigation among them is beyond the scope of the current study. This study uses the first-order bounding approach (Cornell 1967) to solve the system reliability as described in Eqn (13):

$$\max_{1 \le i \le k}(P_{fi}) \le P_f \le 1 - \prod_{i=1}^{k}(1-P_{fi}), \tag{13}$$

where: P_{fi} is the failure probability of the i^{th} failure modes, P_f is the system failure probability. Although the failure probability of MCS is located within the bounds derived by FORM, it should be cautious about the nonlinearity of the limit state functions. When the limit state function is highly nonlinear, FORM may not be able to deliver a promise failure probability.

The failure probability calculated in this section is used as the conditional probability of the failure probability node in the second part of the BN.

Table 10. Failure probabilities (P_f)* at 15 bridge sites from stability-based reliability

Bridge	1	2	3	4	5	6	7	8	9	10	11	12	13	14	15
P_f^{**}	0.28	0.40	0.19	0.38	0.16	0.47	0.10	0.36	0.35	0.35	0.41	0.57	0.20	0.20	0.19
C_r^{***}	1.60	1.22	2.06	1.28	2.29	1.06	3.00	1.33	1.36	1.36	1.20	0.87	2.00	2.00	2.06
P_f^{****}	~0														

*Per hundred years; **with scouring potential; ***(%); ****no scouring potential.

Table 11. Failure probabilities at bridge No.8 calculated by MCS and FORM

Approach	P_f
MCS	0.36
FORM	0.27–0.39

4. Results of the PIEF and BN evaluation

The 15 bridge sites over the Gaoping River are first assessed using the existing PIEF (Table 1). The established BN is then used for the reliability analysis, and the correlation between the two is analyzed. The evaluation results using the PIEF and BN are displayed in Table 12. The highest PIEF rating was attained by Bridge No. 13 (33.86). According to the PIEF standard, this bridge had a medium level of scouring potential (50–25). Bridge No. 1 had the lowest rating (12.01), which is a low scouring potential (<25). Table 13 shows the average estimated PIEF scores based on location. Bridges on the upstream area of the basin had higher scores than those on the downstream area. This was because bridges on the upstream area were more likely to: (1) have a dam; (2) be located at river bends or contractions; (3) have greater eroded river bed; (4) have more significant hydraulic drop effect.

Table 12. Results of PIEF and BN posterior probability at each bridge sites

Bridge No.	PIEF score potential	Prior BN Scour potential (%)	Posterior Failure Prob.*
No. 1	12.01	5.18	0.132
No. 2	19.96	22.17	0.286
No. 3	15.96	16.14	0.126
No. 4	18.25	14.71	0.258
No. 5	12.48	7.32	0.253
No. 6	24.58	35.59	0.392
No. 7	18.27	11.78	0.080
No. 8	29.93	39.82	0.333
No. 9	30.28	45.50	0.379
No. 10	21.57	33.26	0.425
No. 11	15.37	11.58	0.262
No. 12	28.46	30.63	0.484
No. 13	33.86	51.97	0.214
No. 14	20.02	10.19	0.112
No. 15	31.16	41.05	0.294

*Against a 100-year flood.

Table 13. Average score of the PIEF results (by location)

Locations	Average Score
Qishan River	25.77
Laonong River	23.15
Gaoping River	16.54

Although Bridge No. 14 was located on the upstream area (Fig. 3), it was not seriously damaged during Typhoon Morakot (2009). The field investigation found that although the bridge was not far from Bridge No. 15, the outcomes of the two bridges during Typhoon Morakot were different. The possible reasons for the different outcomes were that the bridge piers did not significantly block the water and that the bridge was neither adjacent to a dam nor located along a bend on the river. The PIEF score of Bridge No. 14 was 20.02, indicating that it had low scouring potential and that the PIEF can reflect the bridge scour potential correctly.

Bridge No. 9 was located on the upstream area of the Laonong River (Fig. 3) and was a newly built, large span steel truss bridge with only one pier on the main river channel (Fig. 13). Based on these characteristics, the scour potential of this bridge should not be high; however, its PIEF score was 30.28 (assuming that it had a pile foundation), indicating that it had medium scouring potential. The major contribution of the score came from the item of effective pier diameter. This result is inconsistent with the idea of a long span bridge. Bridges with a single pier with large diameter result in a high PIEF score, which is clearly not reasonable. This indicates that the PIEF can still be improved.

Fig. 13. Picture of bridge No. 9

Figure 14 illustrates the relationship between the network prior scouring potential and the PIEF results. These two results were positively correlated with a correlation coefficient of 0.938. This indicates that, before updating, the BN successfully reflected the PIEF contents. Figure 14 shows the relationship between the network posterior failure probability and the PIEF results. The correlation coefficient was 0.513. Because the PIEF only focused on the assessment of scouring potential, a lower coefficient of correlation was expected. Table 13 also revealed that a bridge with a medium scouring potential from the PIEF (Bridge No. 6) was equivalent to a bridge with a probability of failure of 0.392 in a 100-year flood.

5. Revision of the existing PIEF

Although a high correlation between the PIEF score and BN prior scouring potential was observed, it is more important to build a close relationship between the PIEF score and the BN posterior failure probability. To increase this correlation, the weights (α) of the PIEF were adjusted based on the Taguchi method (Weng *et al.* 2008). It should be noted that the first part of the BN was based on the PIEF. Once the weights (α) of the PIEF were adjusted, the BN must be reconstructed accordingly.

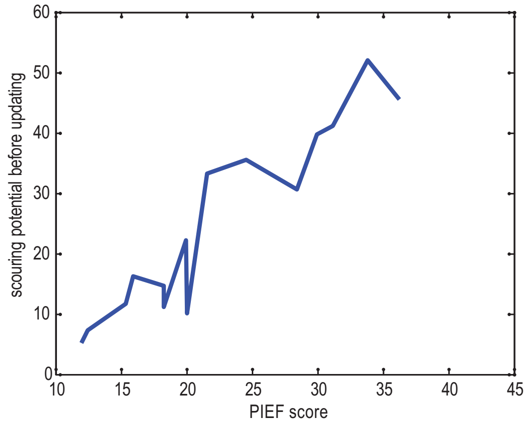

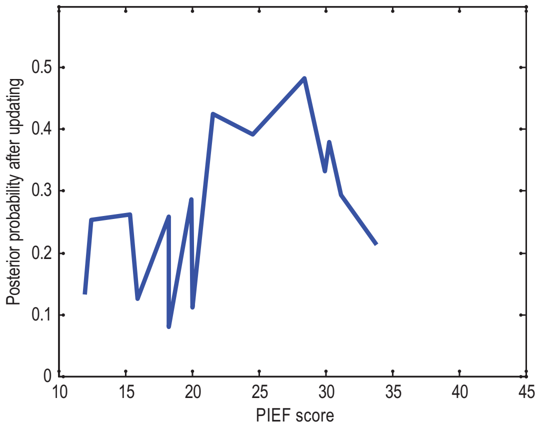

Fig. 14. Relationship between the original PIEF and BN

If trial-and-error approach is used for identifying the optimal weights in the PIEF, according to the results of the current experiment, one may adjust the weight value (α) in the next experiment to achieve a higher correlation. The drawback of this strategy is that the obtained weight may not be the optimum and the computational cost is too expensive. A full factorial experiment may deliver the optimal weights. However, its cost is often higher than that of the trial-and-error approach.

To solve the above difficulties, Taguchi approach adopts the concept of orthogonal array (OA) to conduct the experiments, which provides an efficient and systematic way to determine weights so that the highest correlation can be found with only a few experimental runs. "Orthogonal" means a balanced and fair selection of weights in all possible combinations. A more detailed definition of OA is given as follows. Let S be a set of s levels. A matrix A of N rows and k columns with entries from S is said to be an OA with s levels and strength t ($0 \le t \le k$) if in every $N \times t$ sub-array of A, each t-tuple based on S appears exactly the same times as a row (Weng *et al.* 2008).

To characterize the nonlinear effect of each weight (α) on the correlation performance, three levels were used to construct the OA, resulting in a L27 Taguchi array. The fitness function was the inverse of the correlation coefficient between the PIEF score and BN posterior failure probability; that is, the smaller the fitness value, the better the match. The fitness value was converted to the signal-to-noise (*S/N*) ratio (η) in the Taguchi method using the formula described below:

$$\eta = -10\log\,(\text{Fitness}). \tag{14}$$

Hence, a small fitness value results in a large *S/N* ratio. The OA, level values, fitness values and *S/N* ratios were described in Table 14. A Taguchi response table (Table 15) was developed by averaging the *S/N* ratios for each weight and each level using Eqn (15):

$$\overline{\eta}(m,\alpha) = \frac{s}{N} \sum_{i,OA(i,\alpha)=m} \eta_i, \tag{15}$$

where: m is the current considered level number (i.e., m = 1, 2 or 3), α is the weight, s is the total level number (s = 3), N is the number of row in OA (N = 27). The largest *S/N* ratio in each column indicates that the highest correlation is achieved when the weight is fixed at this level. Thus, such level was the optimal level for that weight (Table 15). Each weight was normalized to en-

Table 14. The OA, level values, fitness values and *S/N* ratios

Experiments	Items													Fitness	*S/N*
	1	2	3	4	5	6	7	8	9	10	11	12	13		
1	5	5	4	6	1	3	3	5	3	16	10	3	8	1.953	–2.91
2	5	5	4	6	2	5	5	7	5	20	13	5	10	1.735	–2.39
3	5	5	4	6	3	7	7	9	7	24	16	7	12	1.706	–2.32
4	5	7	6	8	1	3	3	7	5	20	16	7	12	1.798	–2.55
5	5	7	6	8	2	5	5	9	7	24	10	3	8	1.62	–2.10
6	5	7	6	8	3	7	7	5	3	16	13	5	10	1.742	–2.41
7	5	9	8	10	1	3	3	9	7	24	13	5	10	2.102	–3.23
8	5	9	8	10	2	5	5	5	3	16	16	7	12	2.055	–3.13
9	5	9	8	10	3	7	7	7	5	20	10	3	8	1.996	–3.00
10	7	5	6	10	1	5	7	5	5	24	10	5	12	2.135	–3.29
11	7	5	6	10	2	7	3	7	7	16	13	7	8	2.037	–3.09
12	7	5	6	10	3	3	5	9	3	20	16	3	10	1.988	–2.98
13	7	7	8	6	1	5	7	7	7	16	16	3	10	1.819	–2.60
14	7	7	8	6	2	7	3	9	3	20	10	5	12	1.717	–2.35
15	7	7	8	6	3	3	5	5	5	24	13	7	8	1.986	–2.98
16	7	9	4	8	1	5	7	9	3	20	13	7	8	2.045	–3.11
17	7	9	4	8	2	7	3	5	5	24	16	3	10	1.879	–2.74
18	7	9	4	8	3	3	5	7	7	16	10	5	12	2.178	–3.38
19	9	5	8	8	1	7	5	5	7	20	10	7	10	1.984	–2.98
20	9	5	8	8	2	3	7	7	3	24	13	3	12	1.958	–2.92
21	9	5	8	8	3	5	3	9	5	16	16	5	8	2.124	–3.27
22	9	7	4	10	1	7	5	7	3	24	16	5	8	2.34	–3.69
23	9	7	4	10	2	3	7	9	5	16	10	7	10	2.408	–3.82
24	9	7	4	10	3	5	3	5	7	20	13	3	12	2.357	–3.72
25	9	9	6	6	1	7	5	9	5	16	13	3	12	2.315	–3.65
26	9	9	6	6	2	3	7	5	7	20	16	5	8	2.705	–4.32
27	9	9	6	6	3	5	3	7	3	24	10	7	10	2.042	–3.10

Table 15. Taguchi response table

Levels	Items												
	1	2	3	4	5	6	7	8	9	10	11	12	13
1	–2.67	–2.91	–3.12	–2.96	–3.11	–3.23	–2.99	–3.16	–2.96	–3.14	–2.99	–2.96	–3.16
2	–2.95	–2.91	–3.05	–2.83	–2.98	–2.97	–3.03	–2.97	–3.08	–3.04	–3.05	–3.15	–2.92
3	–3.50	–3.29	–2.94	–3.33	–3.02	–2.91	–3.09	–2.98	–3.08	–2.93	–3.07	–3.01	–3.03
Δ*	0.83	0.39	0.18	0.50	0.13	0.32	0.09	0.20	0.13	0.21	0.08	0.19	0.25
Opt. α	5	7	8	8	2	7	3	7	3	24	10	3	10
final α**	5	7	9	8	2	8	3	7	3	25	10	3	10

* Δ = highest *S/N* – lowest *S/N*; ** the normalized weights.

sure that the sum of the total optimal weights was equal to 100. A confirmation experiment was then performed using each optimal weight. Note that the Taguchi response table also indicated that the items of upstream river dam and the protection for river bed have the largest and smallest effects on the correlation performance, respectively.

Table 15 indicated that weighs (α) of bending of the river, location of the main channel and foundation exposure depth were increased. Remember that experts suggest a special rule for the original PIEF and if it is satisfied, the bridge is considered to have high scouring potential regardless of the overall score. Table 1 illustrated that this special rule is applied to items of eroded river bed, location of the main channel and foundation exposure depth. It is seen that two of these three important items have been suggested to increase their weights in Table 13 (the eroded river bed remains the same). The proposed PIEF emphasizes this experts' opinion by allocating more weight on two corresponding items. Other points about the updated contents in the proposed PIEF are briefly discussed below:

1. The hydraulic drop effect and the protection for river bank were mainly determined by in-situ observations. However, it was not an easy task to determine the values for each item resulting a similar PIEF score between bridges. Thus, these two items did not have a significant impact on the PIEF score. Their weights (α) were then reduced.
2. The roles of area ratio of bridge to cross section and effective pier diameter were similar. The influence of area ratio of bridge to cross section may be overweight, as discussed for Bridge No. 9 in section 4. Hence, weights (α) of the effective pier diameter and area ratio of bridge to cross section were both reduced.

Figure 15 illustrates the relationship between the posterior failure probability of the BN and the PIEF score. The correlation coefficient between the posterior failure probability and the PIEF score was increased to 0.696, indicating the revised PIEF delivered a more promising result.

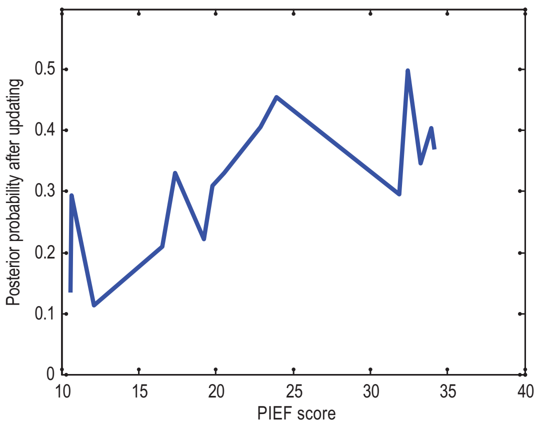

Fig. 15. Relationship between the proposed PIEF and BN

Conclusions

Bridge scour potential is an interdisciplinary problem that involves a wide range of knowledge. To improve the current preliminary assessment procedures used in Taiwan, a BN was constructed on the basis of an existing PIEF to systematically and probabilistically evaluate the scour potential at bridge sites. Historical events were incorporated into the proposed assessment process via Bayesian theory to increase the accuracy of the analysis results. Thus, the established BN has learning capabilities and can update the assessment results according to newly collected data. For practical purposes, the BN analysis results were converted into a PIEF to help engineers implement the relevant operations. In addition, the Taguchi method was used to find the optimal allocated weights for each evaluated item in the proposed PIEF.

This study only considered the uncertainties in the Gaoping River Basin and bridges with pile foundations. Caution should be taken in applying the proposed PIEF to other river basins or foundation types.

Acknowledgements

The authors appreciate financial support from China Engineering Consultants, Inc. in Taiwan.

References

Agena Ltd. 2007. *AgenaRisk software package* [online], [cited 10 Dec 2012]. Available from Internet: http://www.AgenaRisk.com.

Ang, A. H.-S.; Tang, W. H. 1984. *Probability concepts in engineering planning and design. Volume II – decision, risk and reliability*. New York: John Wiley & Sons, Inc. 574 p.

Army Corps of Engineers, Hydrologic Engineering Center. 1997. *HEC-RAS, River analysis system, hydraulic reference manual, version 2.0*. Davis, California. 411 p.

Cesare, M. A. 1991. First-order analysis of open-channel flow, *Journal of Hydraulic Engineering* 117(2): 242–247. http://dx.doi.org/10.1061/(ASCE)0733-9429(1991)117:2(242)

Chang, Y. L.; Chou, N. S. 1989. Chang's simple side pile analysis approach, *Sino-Geotechnics* 25: 64–82.

Chen, C. C.; Chan, Y. W.; Tian, Y. C.; Chang, G. C.; Li, H. Y.; Wang, C. L.; Li, Y. L. 1996. *Highway bridge testing and evaluation*. Taiwan: Taiwan Construction Research Institute. 55 p.

Cornell, C. A. 1967. Bounds on the reliability of structural systems, *Journal of the Structural Division* 93(1): 171–200.

Fischenich, C.; Landers, M. 1999. *Computing Scour, EMRRP technical notes collection (ERDC TN-EMRRP-SR-05)*. Vicksburg: U.S. Army Engineer Research and Development Center. 4 p.

Ghosn, M.; Wang, J. 2003. Reliability model for bridge scour analysis, in *Proc. of the third IABMAS Workshop on Life-Cycle Cost Analysis and Design of Civil Infrastructures Systems*, 2003, Lausanne, Switzerland, 238–246.

Jain, S. C. 1981. Maximum clear-water scour around cylindrical piers, *Journal of the Hydraulics Division* 107(5): 611–625.

Jain, S. C.; Ficher, E. E. 1980. Scour around bridge piers at high flow velocities, *Journal of the Hydraulics Division* 106(11): 1827–1842.

Johnson, P. A. 1992. Reliability-based pier scour engineering, *Journal of Hydraulic Engineering* 118(10): 1344–1358. http://dx.doi.org/10.1061/(ASCE)07339429(1992)118:10(1344)

Johnson, P. A. 1995. Comparison of pier scour equations using field data, *Journal of Hydraulic Engineering* 121(8): 626–629.
http://dx.doi.org/10.1061/(ASCE)0733-9429(1995)121:8(626)
Johnson, P. A. 1996. Uncertainty of hydraulic parameters, *Journal of Hydraulic Engineering* 122(2): 112–115.
http://dx.doi.org/10.1061/(ASCE)0733-9429(1996)122:2(112)
Johnson, P. A. 1999. Fault tree analysis of bridge failure due to scour and channel instability, *Journal of Infrastructure Systems* 5: 35–41.
http://dx.doi.org/10.1061/(ASCE)1076-0342(1999)5:1(35)
Johnson, P. A.; Ayyub, B. M. 1992. Assessing time-variant bridge due to pier scour, *Journal of Hydraulic Engineering* 118(6): 887–903.
http://dx.doi.org/10.1061/(ASCE)0733-9429(1992)118:6(887)
Johnson, P. A.; Dock, D. A. 1998. Probabilistic bridge scour estimates, *Journal of Hydraulic Engineering* 124(7): 750–755.
http://dx.doi.org/10.1061/(ASCE)0733-9429(1998)124:7(750)
Li, T. C.; Liu, J. B.; Liao, Y. J. 2011. A discussion on bridge-closure according to the water stage, *Sino-Geotechnics* 127(1): 79–86.
Mays, L. W.; Tung, Y.-K. 1992. *Hydrosystems engineering and management*. New York: McGraw-Hill Book Co., Inc. 550 p.
Melchers, R. E. 2002. *Structural reliability analysis and prediction*. Chichester: John Wiley and Sons. 456 p.
Ministry of Economic Affairs. 2008. *Regulation Master Plan of Gaoping River.* Water Resources Agency, Taipei, Taiwan. 35 p.
Ministry of Transportation and Communications. 2009. *The bridge design specifications.* Taiwan: Ministry of Transportation and Communications. 58 p.
Muzzammil, M.; Siddiqui, N. A.; Siddiqui, A. F. 2008. Reliability considerations in bridge pier scouring, *Structural Engineering and Mechanics* 28(1): 1–18. http://dx.doi.org/10.12989/sem.2008.28.1.001
Naess, A.; Leira, B.; Batsevych, O. 2009. System reliability analysis by enhanced Monte Carlo simulation, *Structural Safety* 31(5): 349–355. http://dx.doi.org/10.1016/j.strusafe.2009.02.004
Neill, C. R. 1965. Measurements of bridge scour and bed changes in a flooding sand-bed river, in *Proc. of the Institution of Civil Engineers*, 1965, London, UK, 415–436.
Palmer, R.; Turkiyyah, G. 1997. *An expert system for the cataloging and expert evaluation of scour risk and river stability at bridge sites*. University of Washington, Washington, USA. [online], [cited 12 Dec 2013]. Available from Internet: http://www.ce.washington.edu/~scour/.
Railway Technical Research Institute (RTRI). 2007. *A technique to extract souring-apprehended bridge piers* [online], [cited 12 Dec 2013]. Available from Internet: http://www.rtri.or.jp/eng/rd/seika/2007/01/safety_E03.html.
Sheen, S. W. 2012. Flood frequency analysis of watersheds in Taiwan, *Journal of Soil and Water Conservation Technology* 7(1):11–21.
Shen, H. W.; Shneider, V. R.; Karaki S. S. 1966. *Mechanics of local scour*. Colorado State University, Fort Collins, Colorado, USA. 57 p.
Shen, H. W.; Shneider, V. R.; Karaki, S. S. 1969. Local scour around bridge piers, *Journal of the Hydraulics Division* 95: 1919–1940.
Tung, Y. K. 1990. Mellin transform applied to uncertainty analysis in hydrology/hydraulics, *Journal of Hydraulic Engineering* 116(5): 659–674.
http://dx.doi.org/10.1061/(ASCE)0733-9429(1990)116:5(659)
U.S. Department of Transportation. 2012. *Evaluating scour at bridges, Hydraulic Engineering Circular No. 18.* 5th ed. Federal Hwy. Administration (FHWA), Washington, D.C., USA. 340 p.
U.S. Department of Transportation. 2001a. *Stream stability at highway structures, Hydraulic Engineering Circular No. 20.* 3rd ed. Federal Hwy. Administration (FHWA), Washington, D.C., USA. 328 p.
U.S. Department of Transportation. 2001b. *Bridge scour and stream instability countermeasures – experience, selection, and design Guidelines, Hydraulic Engineering Circular No. 23.* 2nd ed. Federal Hwy. Administration (FHWA), Washington, D.C., USA. 400 p.
Wang, C. K. 2002. *Characteristics of local scour around non-uniform piers with collar protection*. Master thesis. Taiwan: National Central University.
Weng, W. L.; Yang, F.; Chang, A. E. 2008. *Electromagnetics and antenna optimization using Taguchi's method.* 1st ed. Morgan & Claypool Press, CA, USA. 15 p.
Wu, R. B.; Yang, J. C.; Yen, B. C.; Lu, J. H. 2001. Study on evaluation of rating curve for Kaoping river, in *Proc. of the 12th Conference of Hydraulic Engineering*, 2001, Tainan, Taiwan, 1–9.
Yanmaz, A. M. 2003. Reliability simulation of scouring downstream of outlet facilities, *Turkish Journal of Engineering & Environmental Sciences* 27: 65–71.
Yeh, K. C.; Tung, Y. K. 1993. Uncertainty and sensitivity analyses of pit-migration model, *Journal of Hydraulic Engineering* 119(2): 262–283.
http://dx.doi.org/10.1061/(ASCE)0733-9429(1993)119:2(262)
Zhao, Y. G.; Zhong W. Q.; Ang, A. H.-S. 2007. Estimating joint failure probability of series structural systems, *Journal of Engineering Mechanics* 133(5): 588–596.
http://dx.doi.org/10.1061/(ASCE)0733-9399(2007)133:5(588)

Kuo-Wei LIAO. Assistant Professor Liao holds a PhD (2004) and an M.S. (1994), both in civil and environmental engineering from University of Illinois at Urbana-Champaign and National Taiwan University, respectively, and a B.S. (1992) in agricultural engineering from National Taiwan University. Dr. Liao has research interests in reliability analysis and reliability-based design, multi-disciplinary optimization, earthquake engineering and statistical machine learning.

Hu-Jhong LU. Mr. Lu is a research assistant and PhD student in the department of construction engineering at National Taiwan University of Science and Technology. He received his M.S. (2007) in civil engineering from Tamkang University.

Chung-Yue WANG. Professor Wang holds a PhD in aerospace engineering and engineering mechanics from University of Texas at Austin (1989), an M.S. in civil and environmental engineering from University of Wisconsin at Madison (1984) and a B.S. in civil engineering from National Cheng-Kung University (1980). Dr Wang has research interests in nondestructive evaluation, bridge engineering, fluid-structure interaction analysis, mechanics of composite materials and motion analysis of structures.